Defence Science Journal, Vol. 68, No. 3, May 2018, pp. 251-259, DOI : 10.14429/dsj.68.11635

Evaluating Impact Resistance of Aluminum 6061-T651 Plate using Smoothed Particle Hydrodynamics Method

Ehsan Hedayati* and Mohammad Vahedi

Department of Mechanical Engineering, College of Technical Engineering, Islamic Azad University, Saveh, Iran
**E-mail: hedayati.uast.ac@gmail.com*

ABSTRACT

Performing various experimental, theoretical, and numerical investigations for better understanding of behavioural characteristics of metals under impact loading is of primary importance. In this paper, application of smoothed particle hydrodynamics (SPH) method in impact mechanics is discussed and effective parameters on impact strength of an aluminum plate are investigated. To evaluate the accuracy of smoothed particle hydrodynamics method for simulating impact, Recht and Ipson model is first provided thoroughly for both Rosenberg analytical model and smoothed particle hydrodynamics method, and then plots of initial velocity-residual velocity and initial velocity-absorbed energy for target of aluminum 6061-T651 are presented. The derived information and simulation results expresses that the maximum error percentage of smoothed particle hydrodynamics method in compared with Rosenberg analytical model is within an acceptable range. Therefore, the results of smoothed particle hydrodynamics method verify the Rosenberg analytical model with high accuracy. Results reveal that higher initial impact velocity decreases the time of projectile penetration, and so penetration depth and length as well as the local damage rate of plate increases.

Keywords: Smoothed particle hydrodynamics; Rosenberg analytical model; Energy absorption; ABAQUS; penetration

1. INTRODUCTION

Application of sheet metal and composites in the industries of aerospace, shipping, car manufacturing, etc. has been largely developed during the recent decades. These sheets which are usually made from steel, aluminum, and composite alloys to be light and strong enough are exploited in the bodies of airplanes, ships, automobiles and other products. One of the most important problems in the mentioned products is their safety against impact and destruction. A practical mechanism for testing sheets safety is determining the extent of sheet damage caused by strike or impact by means of specifying the shape, area, and depth of failure zone. Therefore, predicting the area and depth of sheet damaged zone created by strike and impact has been always among the challenges of engineers and researchers[1]. Today's rapid progress and improvement of computational mechanics techniques made determining strength and useful life as well as predicting fracture much faster and cheaper. In addition, applying these techniques and numerical simulations provides the opportunity for one to change different parameters easily and at low cost to study their effect.

Due to prevalence and importance of impact phenomenon among metallic and composite structures, numerous experimental, numerical and analytical researches have been conducted for studying impact process. Taylor[1] studied the momentary impact between a thin flat-ended cylinder and a rigid wall analytically and could determine the cylinder dynamic yield stress during impact.

Jonas[2], *et al.* simulated the impact of a thin cylinder against a stiffened plate in different angles by finite element method and compared the numerical results with experimental ones. They used the primarily elastic-plastic model for describing material behaviour, and so could not model the experimental results correctly. Belytschko[3], *et al.* presented a new algorithm for simulating three-dimensional impact of two objects and could model the impact between a thin cylinder and a plate. Because of applying elastic-plastic model for predicting material behaviour, results are neither accurate enough nor of good quality.

Holian[4], *et al.* performed a hydrodynamic simulation for hypervelocity impact of a metal bullet with a thin plate. They shown that simulated results are not in relatively good agreement with experimental ones due to application of primarily elastic-plastic model. Meier[5] simulated the impact of a metal ball against a composite plate. He is able to accurately model the plate perforation by applying Eulerian method.

Chou[6], *et al.* studied the penetration of a bar into a plate once analytically and once by finite element simulation method. They took advantage of Johnson–Cook elasto-plastic model for material behaviour and could simulate the bar penetration into the surface to some extent. Schonberg[7], *et al.* parametrically investigated the hypervelocity impact of a cylindrical projectile with a thin plate. They used Mie-Gruneisen equation of state for describing material behaviour and could simulate the projectile

Received : 16 July 2017, Revised : 17 October 2017
Accepted : 11 December 2017, Online published : 16 April 2018

penetration into the plate, being in agreement to some extent with experimental results[7].

Jenq[8], *et al.* analytically investigated the impact of a round nose cylindrical projectile with a composite flat plate. They considered the degradation of material properties and revealed that without including degradation of material properties, appropriate results cannot be obtained. Nandlall[9], *et al.* modelled the impact of a sharp cylindrical projectile against a plate. In this model, they could simulate the plate perforation with appropriate accuracy by using Matznemiller damage model .

Kruse[10], *et al.* studied the impact of a projectile with a thin plate experimentally and analytically. They investigated the effect of various parameters on shape of damage zone. Lee[11] simulated the impact of long cylinder with stationary and moving oblique plates two-dimensionally. They applied Johnson–Cook elasto-plastic model and to some extent could demonstrate the results of cylinder penetration into the plate.

Borvik[12], *et al.* performed a 2D simulation for impact of projectiles with flat, hemispherical and conical noses against a thick steel plate. They used Johnson-Lindholm fracture model and could appropriately present the results of penetration and perforation of projectile into the plate. Guo[13], *et al.* simulated the impact of projectiles with flat, hemispherical and conical noses against a thick aluminum plate three-dimensionally. In this study, applying the shear fracture model, they could model the perforation of the projectile through plate to a large extent. Gu[14], *et al.* performed a 3D simulation for impact between a conical nose projectile and a composite plate. In this study, due to application of primarily elastic-plastic model, the simulation results are not appropriate and in agreement with the provided results .

Using Eulerian method, Scheffler[15] conducted a 3-D simulation for impact of a conical–nose projectile with an aluminum plate. He applied Johnson–Cook model in this simulation and proved that by applying Eulerian method, no one can obtain as accurate results as experiments. Teng[16], *et al.* simulated the perforation and penetration of a flat projectile into a plate two-dimensionally. They took six different fracture models for describing the material behaviour into account and compared the results with each other.

Song[17], *et al.* simulated the impact between a projectile and stiffened plates three-dimensionally. They used fracture strain for modelling fracture behaviour of material and predicted the fracture areas with an acceptable accuracy. Rashid[18], *et al.* carried out a 3-D simulation for impact of a flat projectile against a composite plate. In this study, due to application of a non-local damage model, simulations show a good agreement with experimental results[18].

Iqbal[19], *et al.* performed a 3-D simulation for impact of a projectile against a thin aluminum plate. Applying Johnson–Cook elasto-plastic model, they could demonstrate the results of the projectile penetration into the plate in different angles with relatively fair accuracy. Babaei[20], *et al.* conducted a 3D simulation for impact between a blunt nosed projectile and multi-layered plate. They utilised the Johnson–Cook elasto-plastic model and could demonstrate the results of projectile penetration into the plate with an acceptable accuracy. Kidane[21], *et al.* simulated the impact of steel ball with aluminum plate three-dimensionally and could predict the plate perforation with appropriate accuracy by using meshless method.

Considering the above studies along with numerous other researches, it seems that understanding the behaviour exhibited by metal composites under ballistic impact demands more precise and in-depth studies. Experimental, analytical, and numerical approaches should be followed when investigation and analysis of penetration phenomenon into metal target is taken into account. Due to their high reliability, experimental methods are the most appropriate ones for such a purpose; however, these methods fail to give information about loading history and the changes introduced during the course of penetration process, while being well expensive. Provided a good agreement between results of analytical method with experimental or numerical data, one can confirm the validity of analytical methods[1,2].

Finite difference or finite volume methods are currently regarded as one of the appropriate methods for analysis of penetration problems, especially those into metallic targets, given their ability to solve all governing equations in continuous media and reduce the computational time and cost as well as their application in complicated problems. Despite being highly successful, grid-based numerical methods have disadvantages limiting their application in complex problem and those characterised by large deformation[22,23].

The grid-less method of SPH has been introduced recently to be applied in various fields of fluid or solid mechanics problems. Smoothed particle hydrodynamics method has achieved widespread popularity for solving free surface problems and those associated with discontinuities and large displacements[22-24].

For investigating the impact strength of aluminum 6061-T651, numerical and analytical studies on failure of aluminum with 10 mm thickness under perpendicular impact loading are conducted in this study by applying smoothed particle hydrodynamics method and commercial software ABAQUS is used for simulating this phenomenon and its caused fracture and failure.

2. SMOOTHED PARTICLE HYDRODYNAMICS METHOD

Smoothed particle hydrodynamics (SPH) method is based on expressing the numerical value of nodes as weighted average over the numerical values of the neighbour nodes. The advantage of this method over the finite element method is its ability to simulate medium with complex geometries and inhomogeneous nodes distribution[22].

SPH method in the realm of stress analysis problems or so on includes spreading finite nodes over the considered problem environment and converting continuous problem to a discretised one into the mentioned nodes. These nodes are accelerating and moving due to their applied hydrostatic pressure or effective stress. By means of a special function, known as smoothing function, which is required to have the following properties, effect of each node on its neighbour nodes is revealed. The previously mentioned properties of smoothing function include[23]:

- Weight function is always positive in the smoothing domain $\widehat{W}(x,h)>0=0$
- Weight function is always zero outside the smoothing domain $\widehat{W}(x,h)>0=0$.
- Weight function is unity $\int_{\Omega}\widehat{W}(x,h)dx=1$.
- Wight function is bell-shaped.
- As smoothing domain (h) approaches zero, weight function approximates to Dirac delta function $\widehat{W}(x,h)>0$

where $\widehat{W}$ is smoothing function or weight function, h is a parameter determining the effective (or smoothing) domain of function and (Ω) is problem domain. All properties of interest in the problem, including stress, pressure, density, etc. are linked to each other by this function[23]. SPH method takes advantage of the integral representation of functions. To describe this approach, function $u(x)$ is defined for each point $X=(x,y,z)$. Integral representation of this function is as shown in Eqn. (1)[24]:

$$u(x)=\int_{-\infty}^{+\infty}u(x')\delta(x-x_i)dx' \tag{1}$$

In this relation, δ is Dirac delta function. Solving Eqn. (1) for entire space is too difficult and so Gingold and Monaghanz rewrote this equation in the approximate form of Eqn. (2) by confining the equation to problem domain Ω and converting Dirac delta function to another function[24]:

$$\langle u(x)\rangle=\int_{\Omega}u(x)W(x-x_i,h)dx \tag{2}$$

where $\langle u(x)\rangle$ is approximate function, $W(x-x_i,h)$ is smoothing function, and h is smoothing length in SPH method. It can be proved that the adopted approximation in SPH method is of second order accuracy[24].

3. PROBLEM MODELLING USING SMOOTHED PARTICLE HYDRODYNAMICS

The projectile was selected to be made of 4340 steel, with the target body (plate) being a 100 mm x 100 mm x 10 mm square plate made of aluminum 6061-T651; moreover, the target body was taken to be supported rigidly and fixed at all four sides (all degrees of freedom were equal to zero). Figure 1 show the model boundary conditions. Plasticity model and Johnson-Cook (J-C) failure model were used for modelling and simulating the projectile and the aluminum plate. J-C model expresses yield stress as in Eqn (3)[25]:

$$\sigma=\left[A+B\varepsilon^{N}\right]\left[1+CIn\dot{\varepsilon}^{*}\right]\left[1-T^{*M}\right] \tag{3}$$

where ε is equivalent plastic strain; $\dot{\varepsilon}^{*}=\dot{\varepsilon}/_{\dot{\varepsilon}_0}$ is dimensionless strain rate; $\dot{\varepsilon}_0=1s^{-1}$; T^{*} is homologous temperature and can be calculated as $T^{*}=T-T_r/T_m-T_r$; P is hydrostatic pressure; $0\le T^{*}\le 1$; A and B are dynamic yield stress and stiffness constant, respectively; and N, M, and C are material constants. Even though this model is an empirical one, it is well flexible and powerful and accounts for the effects of important parameters. As the temperature approaches toward melting point $(T^{*}=1)$, strength tends to zero. J-C model is based on damage accumulation, i.e., as the element fails as the damage reaches $D=1$. Following the failure, the material behaves as a liquid as it has no strength (no shear and deviatory stress) and is unable to generate any hydrostatic tensile stress, being only capable of bearing hydrostatic pressure. Moreover, an increase in damage may end up with a gradual decrease in strength, making the material so-called 'soft'. Damage to an element can be written as

$$D=\sum\frac{\Delta\varepsilon_p}{\varepsilon_p^{f}} \tag{4}$$

where the nominator represents equivalent plastic strain rate and denominator is equivalent strain-to-failure.

The general expression for strain-to-failure is given by Eqns. (5) and (6)[25]:

$$\varepsilon_p^{f}=\left[D_1+D_2\exp\left(D_3\sigma^{*}\right)\right]\left[1+D_4In\dot{\varepsilon}^{*}\right]\left[1+D_5T^{*}\right]\sigma^{*}\le 1.5 \tag{5}$$

$$\varepsilon_p^{f}=\left[D_1+D_2\exp\left(1.5D_3\right)\right]\left[1+D_4In\dot{\varepsilon}^{*}\right]\left[1+D_5T^{*}\right]\sigma^{*}>1.5 \tag{6}$$

where $\sigma^{*}=\sigma_m/\sigma$ is the dimensionless stress-pressure ratio, σ_m is the average of the three principal normal stresses, $\bar{\sigma}$ is von Mises equivalent stress, $\dot{\varepsilon}^{*}$ is dimensionless strain rate, and T^{*} is homologous temperature.

The projectile is depicted in Fig. 1, with the mechanical characteristics and equations of state of the projectile and target being presented in Table 1[26-31].

4. NUMERICAL MODEL VERIFICATION

In the course of the process through which the projectile penetrates into the target, considering the target material and geometrical parameters of the projectile, part of initial kinetic

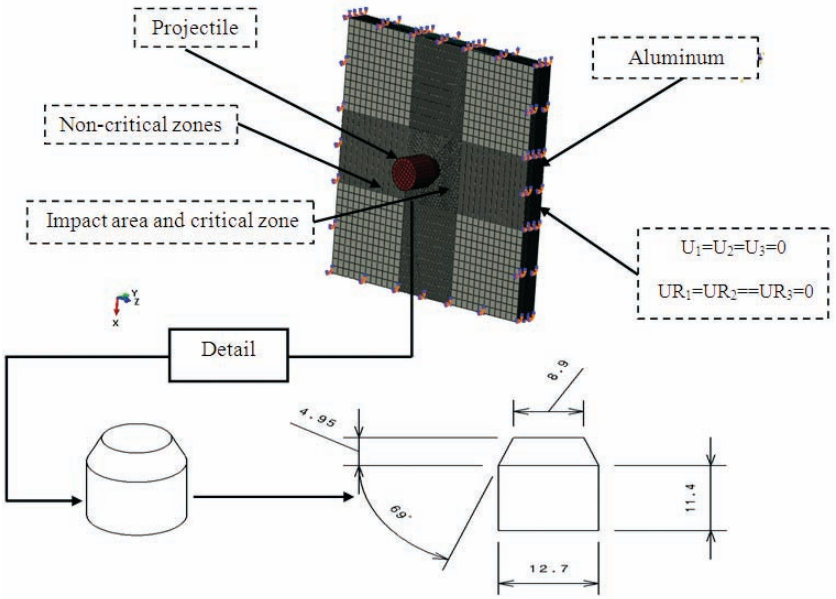

Figure 1. A schematic presentation of the model boundary conditions, 3D solid element meshes used in the numerical simulations and Schematic geometry of the projectile[26].

Table1. Mechanical properties and Johnson-Cook model parameters for the materials[27-31].

Mechanical properties, Johnson-Cook model parameters	Al6061-T651	Steel 4340
Density, (kg/cm^3), ρ	2703	7850
Young's modules,(GPa), E	68.9	200
Poisson ratio, ϑ	0.33	0.29
Yield stress (MPa), σ_y	276	710
Ultimate stress, (MPa), σ_{uts}	310	1110
Specific heat, (J/Kg/°C)	885	477
Elongation at break, $\%, \varepsilon_f$	17	13.2
Reference strain rate, $\dot{\varepsilon}_0$	0	0.15
A [MPa]	262	1430
B [MPa]	161.2	2545
n	0.2783	0.7
C	0	0.014
m	1.34	1.03
T_m(°C)	925	1793
T_0(°C)	293.2	293.2
Initial failure strain, D_1	-0.77	0.05
Exponential factor, D_2	1.45	3.44
Triaxiality factor, D_3	0.47	2.12
Strain rate factor, D_4	0	0.002
Temperature factor, D_5	1.6	0.61

energy of the projectile is absorbed by the target. As such, a structure can serve as an energy absorber when it is capable of tolerating maximum stress at which it can exhibit maximum strain or deformation. So, calculation of residual velocity of a projectile is of paramount importance when it comes to impact modelling. Since Recht-Ipson model is in good agreement with experimental results, In order to calculate post-damage residual velocity of rigid projectiles in any plate (i.e. metallic, composite-made, ceramic, etc.), one can use Recht and Ipson model; this analytical model is expressed as Eqn (7)[32]:

$$\frac{M_p V_o^2}{2} = \frac{M_p V_r^2}{2} + W \tag{7}$$

where M_p is the projectile mass, V_0 and V_r are impact velocity and residual velocity of the projectile, respectively, and W denotes the work performed at target (at full penetration).

This performed work is, indeed, equal to the absorbed energy. Ballistic limit velocity of the projectile, V_{bl}, in the Recht and Ipson analytical model is expressed by Eqn. (8) [32]:

$$V_{bl} = \left(V_o^2 - V_r^2\right)^{0.5} \tag{8}$$

It is extremely difficult to propose a simple analytical penetration model based on time and stress strength variations. Instead, Rosenberg defined the effects of stress-strength for a metallic target under a projectile penetration. This analytical model expresses the effects of stress-strength in penetration and damage phenomena considering the performed work. Therefore, one may refer to Eqn. (9) to calculate the performed work[32]:

$$W = \pi r^2 \sigma_r H \tag{9}$$

where r is the projectile radius, H is target thickness, and σ_r is the stress strength. Therefore, Rosenberg[32], *et al.* used Eqn. (8), which expresses the Recht and Ipson model, to define the value of ballistic limit velocity as Eqn. (10):

$$V_{bl} = \left(\frac{2\sigma_r H \pi r^2}{M_p}\right)^{0.5} \tag{10}$$

$$M_p = \pi r^2 \rho_p L_{eff} \tag{11}$$

where M_p, ρ_p, and L_{eff} denote mass, density, and effective length (total length) of the projectile. Furthermore, Rosenberg and Dekel[32] presented Eqn. (12) for calculating stress strength (σ_r) based on constant $\frac{H}{D}$:

$$\frac{\sigma_r}{Y} = 2\,\frac{1}{3} < \frac{H}{Y} < 1 \tag{12}$$

where D is the projectile diameter and Y is dynamic yield stress.

4.1 Comparison of Simulation Results and Factors Affecting Impact Strength of the Plate with Analytical Models

4.1.1. Trend of Solution Convergence of Numerical Model based on Mesh Size

Considering Fig. 1, critical and non-critical zones of the target body and projectile were meshed used the 3-dimensional elements of PC3D, C3D8, and C3D8, respectively. These elements have eight nodes and each node has three degrees of freedom along the *X, Y, Z* directions. They are used for non-linear elasto-plastic analyses and plastic deformations [33]. The elements should be considered not only in terms of shape, but also in terms of size. For this purpose, one should investigate convergence of solutions, which is an essential issue that ensures accuracy of the results. When investigating convergence of solutions, which contributes to higher accuracy as the elements become finer, it should be noted that only elements within critical zones of the model should become finer. Therefore, in the aforementioned model, only critical zone of the target is subjected to element size change, with the size of elements within non-critical zones of the target and projectile been assumed to be fixed and unchangeable.

To observe the trend of solution convergence of the model, element size across the critical zone was varied according to Table 2, while size of the elements across non-critical zone and projectile were assumed to be 3 mm and 1.5 mm, respectively. According to Table 2, it is seen that, for element sizes of 0.6 mm, 0.55 mm, 0.5 mm, and 0.45 mm, the solutions converged. As such, the 0.60 mm was selected as the optimum element size across the critical zone of the model as the time to solve the problem would be shorter than that with an element size of 0.45 mm while the resulting difference in the solutions was negligible.

4.1.2 Trend of Impact and Damage to Plate

Aiming at demonstrating the general trend of changes leading to structure damage under the effect of an impact, Fig. 2 demonstrate an example of the trend of structural damage

Table 2. Trend of solution convergence of numerical model based on mesh size.

Element size across the non-critical zone (mm)	Element size the across projectile (mm)	Element size across the critical zone (mm)	Maximum value of von mises stress (Mpa)	Convergence and divergence for simulation results
3	1.5	2	411.5	
3	1.5	1	434.3	Divergence
3	1.5	0.90	424.7	
3	1.5	0.75	422.2	
3	1.5	0.60	435.4	
3	1.5	0.55	433.7	Convergence
3	1.5	0.50	431.1	

for initial projectile velocity of V_0= 420 m/s within different time intervals, as extracted using SPH method.

4.1.3 Projectile Velocity Changes and Penetration Time

This section investigated the changes in projectile velocity and penetration time to the target body, with a discussion presented on factors affecting these parameters. Since in the present research, the impact happens at high speed, the projectile will leave the structure at a residual velocity. In this modelling, initial projectile velocity is the most affective factor on penetration time and the velocity at which the projectile leaves the structure.

To thoroughly present the Recht and Ipson model for the Rosenberg analytical model and SPH method, Considering the Eqns. (7), (8), and (10), according to Figs. 3 and 4, the plots of data on initial velocity-residual velocity and initial velocity – absorbed energy for the target made of Aluminum 6061-T651 are presented. The data extracted from the above plots and simulation results are presented on Table 3.

Considering Table 3, it is observed that maximum error percentages on residual velocity and absorbed energy in SPH method, when referenced to those of Rosenberg analytical model, were 9.80 per cent and 9.77 per cent, respectively. Acceptable range of error percentage is 6-12 per cent, which is appropriate for concluding on impact behaviour of the mentioned target. Therefore, SPH method-related data confirm residual velocity and absorbed energy values obtained with Rosenberg analytical model at high accuracy.

It is observed that at higher initial velocities, the rate of velocity variations is higher at initial seconds, and the projectile tend to achieve its steady velocity within shorter time. As a result, the higher the initial velocity of the projectile, the shorter will be the time required to penetrate into the target body, reducing the projectile energy accordingly. The information as given in Table 3 is further depicted on Figs. 5 and 6 which compare the trend of changes in residual velocity and projectile energy with reference to its initial velocity.

4.1.4. Damaged Zone Status

Projectile will generate different stress fields into the target body depending on its initial velocity. The following

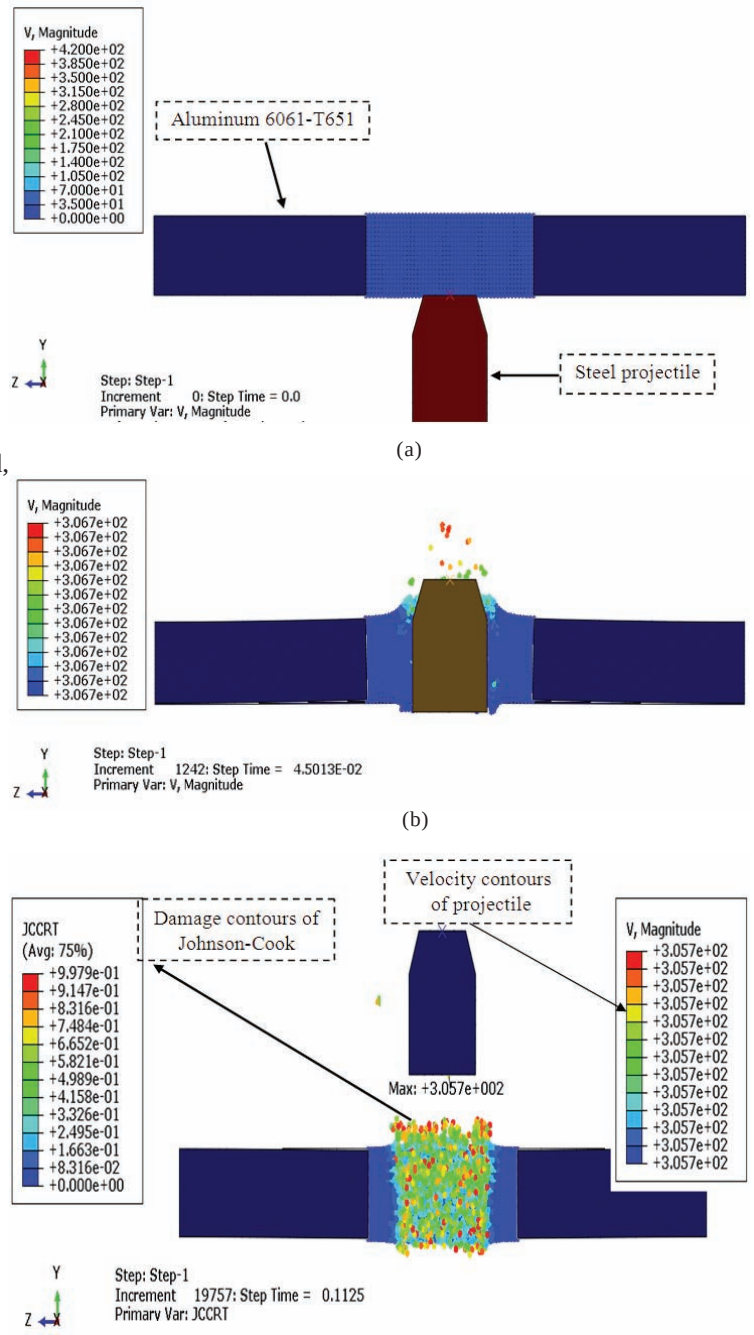

Figure 2. Location of projectile and plate: (a) before strike, (b) after 0.045013 s, and (c) after 0.1125 s.

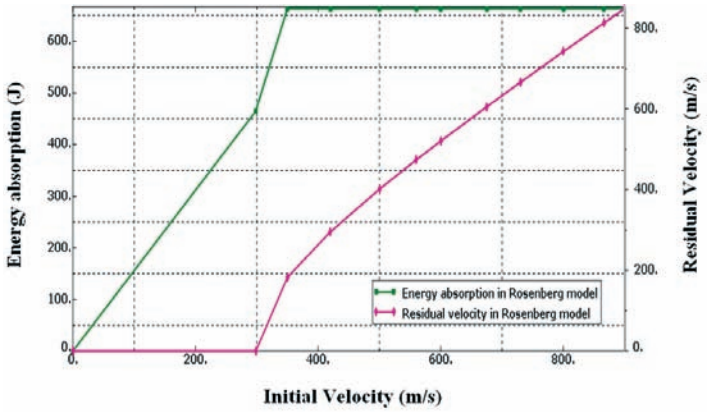

Figure 3. Residual velocity of projectile and absorbed energy at initial velocity using Rosenberg model.

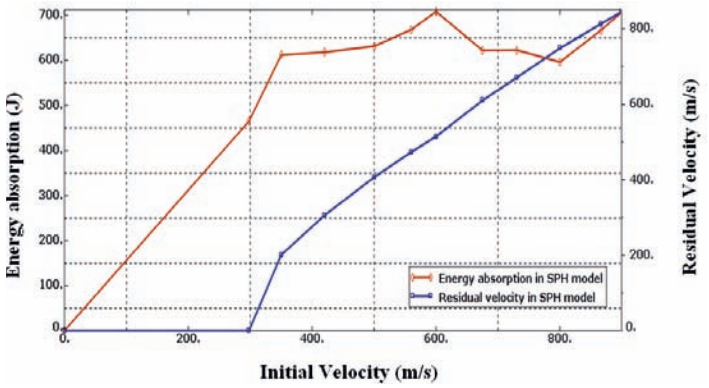

Figure 4. Residual velocity of projectile and absorbed energy at initial velocity using SPH method.

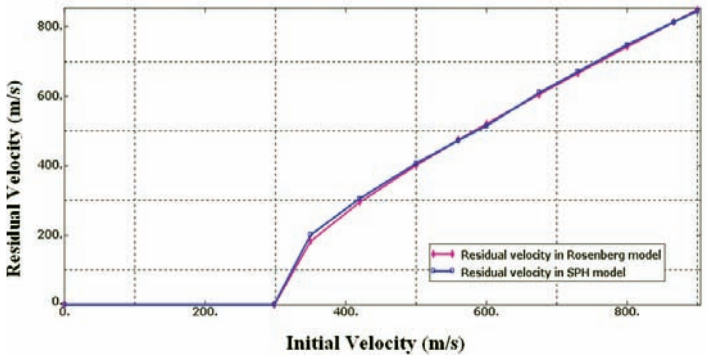

Figure 5. Comparison between residual velocity of the projectile as a function of initial velocity for Rosenberg analytical model and SPH method.

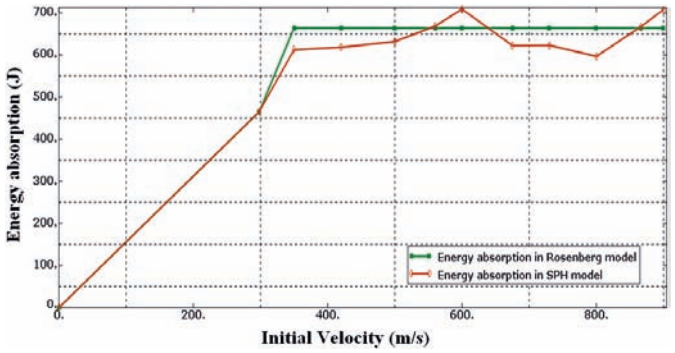

Figure 6. Comparison between absorbed energy as a function of initial velocity for Rosenberg analytical model and SPH method.

figures show the stress distribution at the instant when the projectile leaves the target body for different cases with fully rigid support under different initial velocities. As can be seen from the following Figs. 7, the penetration depths at 350 m/s, 420 m/s, 600 m/s, and 866 m/s were 16.80 mm, 16.76 mm, 17.39 mm, and 30.57 mm, respectively. Furthermore, the penetration length at the mentioned lengths was 13.20 mm, 13.84 mm, 18.08 mm, and 19.06 mm, respectively. The information presented in Fig. 7 are further plotted in Fig. 8, with each plot showing the trend of changes in penetration depth and penetration length into the plate with reference to the initial velocity of the projectile.

The results presented in Figs. 7 and 8 indicate that, with increasing the initial impact velocity, penetration depth and penetration length into the plate increase, enlarging the area across the target body which is affected and damaged by the impact and hence increasing the local damage. Also Increase of projectile velocity and projectile impact velocity with target thus causes pressure area developed in the target to expand. In this condition, projectile impact with target induces impact stresses to spread through target. Therefore, these stresses lead to highly intense pressure variation which ultimately gives rise to increase of penetration length and depth.

5. CONCLUSIONS

In the present study, based on damage growth model, an impact was numerically modeled on aluminum 6061-T651 using SPH method. In this impact modelling, we begin with

Table 3. Residual velocity of projectile as a function of initial projectile velocity for Rosenberg analytical model and SPH method.

	V_r (m/s) Rosenberg))	V_r (m/s) (SPH)	Error (per cent)	SPH (Time required for penetration (s))	$E_{absorbed}$ (Rosenberg)	$E_{absorbed}$ (SPH)	Error (per cent)
866	812.94	812.70	0.02	0.045013	663.45	666.58	0.47
800	742.23	748.10	0.78	0.045017	663.45	598.58	9.77
730	662.30	670.30	0.61	0.067506	663.45	622.80	6.12
600	520.50	514.70	1.11	0.067509	663.45	708.38	6.77
560	473.83	473.20	0.14	0.067604	663.45	668.13	0.70
500	401.15	406.50	1.30	0.067704	663.45	631.44	4.82
420	295.50	305.70	3.40	0.112500	663.45	617.95	6.85
350	182.81	200.90	9.80	0.117000	663.45	611.93	7.76

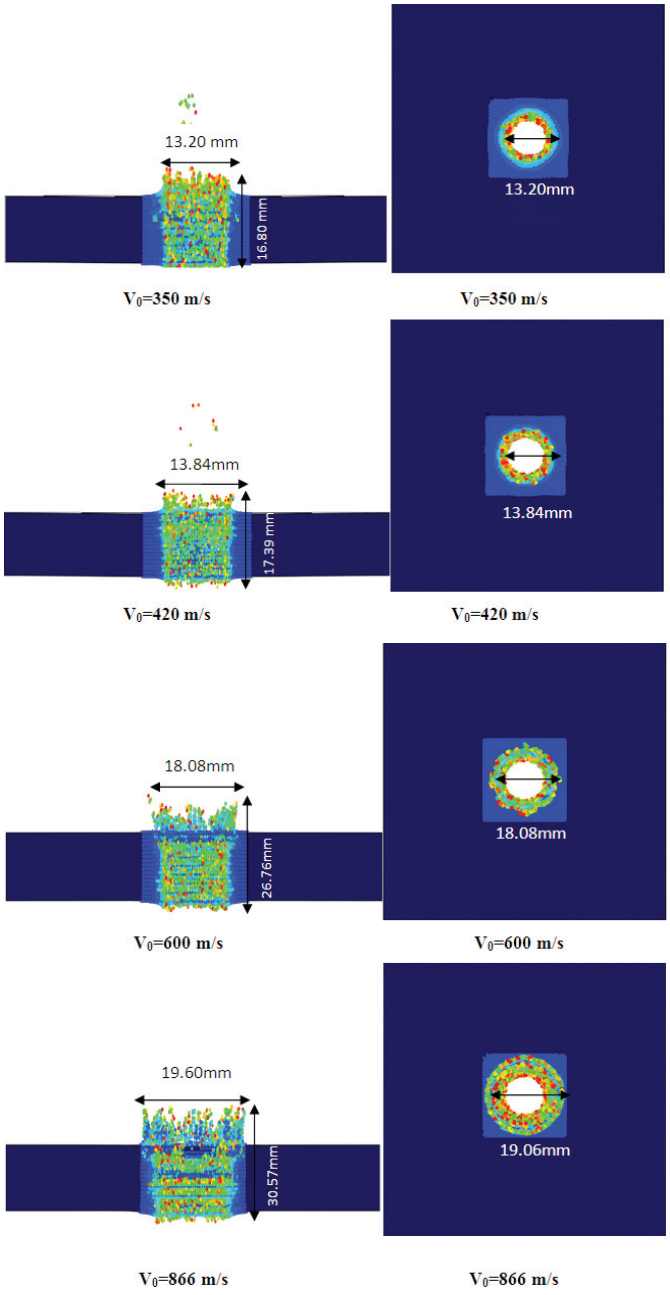

Figure 7. Distribution contours of stress, penetration depth, and penetration length generated in the plate under different initial velocities.

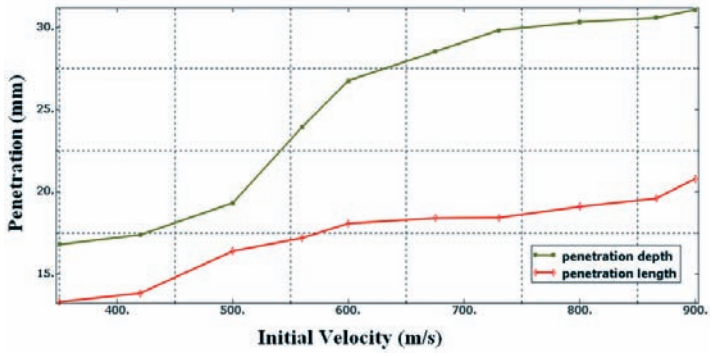

Figure 8. Plot of penetration depth and penetration length at initial velocity using SPH method.

presenting Recht and Ipson model for the Rosenberg analytical model and SPH method. Then, plots of data on initial velocity-residual velocity and initial velocity-absorbed energy were presented for a target made of aluminum 6061-T651. The data extracted from the above plots and simulation results show that maximum error percentages on residual velocity and absorbed energy in SPH method, when referenced to those of Rosenberg analytical model, were 9.80 per cent and 9.77 per cent, respectively. Therefore, SPH method-related data confirm residual velocity and absorbed energy values obtained with Rosenberg analytical model at high accuracy. Furthermore, since the projectile tends to develop different stress fields into the target body depending on its initial velocity, one may see from the results that an almost linear relationship exists between residual velocity of the projectile and initial impact velocity, indicating the fact that, at higher initial velocities, the rate of velocity variations is higher at initial seconds, and the projectile tend to achieve its steady velocity within shorter time. Moreover, with increasing the initial impact velocity, penetration depth and penetration length into the plate (target) increase, enlarging the area across the target body which is affected and damaged by the impact. In this modelling, initial velocity of projectile and boundary conditions were the factors affecting penetration time and residual velocity of the projectile.

REFERENCES

1. Taylor, G. I. The use of flat-ended projectiles for determining dynamic yield stress I. Theoretical considerations. *In* Proceedings of Royal Society of London, England. 1948, **194**(1038), 289–299. doi: 10.1098/rspa.1948.0081.
2. Jonas, G.H. & Zukas. J.A. Mechanics of penetration: Analysis and experiment. *Int. J. Eng Sci.*, 1978, **16** (11) , 879-903. doi : 10.1016/0020-7225(78)90073-3
3. Belytschko, T. & Lin, J.I. A three-dimensional impact-penetration algorithm with erosion. *Int. J. Impact. Eng.*, 1987, **5**(1), 111-127. doi : 10.1016/0045-7949(87)90220-3
4. Holian, K.S. & Holian, B.L. Hydrodynamic simulations of hypervelocity impacts. *Int. J .Impact Eng*., 1989, **8** (2), 115-132. doi: 10.1016/0734-743X(89)90011-0
5. Meier, R.W. Effect of parametric variations of complex target on damage from projectile impact. *Int. J. Impact. Eng.*, 1990, **10** (1-4), 375-387. doi: 10.1016/0734-743X(90)90073-5
6. Chou, P.C.; Hashemi, J.; Chou, A. & Rogers, H.C. Experimentation and finite element simulation of adiabatic shear bands in controlled penetration impact. *Int. J. Impact. Eng.*, 1991, **11**(3), 305-321. doi: 10.1016/0734-743X(91)90041-D
7. Schonberg, W.P. & Peck, J.A. Parametric study of multi-wall structural response to hypervelocity impact by non-spherical projectile. *Comput. Struct*., 1993, **49** (4), 719-745. doi: 10.1016/0045-7949(93)90075-O

8. Jenq, S.T.; Jing, H.S. & Chung, C. Predicting the ballistic limit for plan woven glass-epoxy composite laminate. *Int. J. Impact. Eng.*, 1994, **15**(4), 451-464. doi : 10.1016/0734-743X(94)80028-8
9. Nandlall, D.; Williams, K. & Vaziri, R. Numerical simulation of the ballistic response of grp plates. *Compos. Sci. Tech.*, 1998, **58**(9), 1463-1469. doi: 10.1016/S0266-3538(98)00030-X
10. Kruse, G.R.; Mendes, W.R.; Sommers, W.J.; Weed, R.A.; Nash, K.D. & Mayo, D.V. Testing and simulation of micro derbies from impact with complex targets. *Int. J. Impact. Eng.*, 1999, **23** (1), 489-500. doi : 10.1016/S0734-743X(99)00098-6
11. Lee, M. A numerical comparison of the ballistic performance of unitary rod and segmented-rods against stationary and moving oblique plates. *Int. J. Impact. Eng.*, 2001, **26** (1-10), 399-407. doi : 10.1016/S0734-743X(01)00090-2
12. Borvik, T.; Hopperstad, O.S.; Berstad, T. & Langseth, M. Perforation of 12 mm thick steel plates by 20 mm diameter projectiles with flat. hemispherical and conical noses Part II: numerical simulations. *Int. J. Impact. Eng.*, 2002, **27**(1), 37-64. doi: 10.1016/S0734-743X(01)00035-5
13. Guo, J.; Shi, G.; Wang, Y. & Lu, C. Efficient modeling of panel-like structures in perforation simulations. *Comput. Struct.*, 2003, **81**(1), 1-8. doi: 10.1016/S0045-7949(02)00389-9
14. Gu, J. & Xu, J. Finite element calculation of 4-step 3-dimentional braided composite under ballistic perforation. *Compos. B. Eng.*, 2004, **35**(4), 291-297. doi: 10.1016/j.compositesb.2004.01.001
15. Scheffler, D.R. Modeling non-eroding perforation of an oblique aluminum target using the eulerian CTH hydrocode. *Int. J. Impact. Eng.*, 2005, **32**(1-4), 461-472. doi: 10.1016/j.ijimpeng.2005.04.008
16. Teng, X. & Wierzbicki, T. Evaluation of six fracture models in high velocity perforation. *Eng. Fract. Mech.*, 2006, **73** (12), 1653-1678. doi: 10.1016/j.engfracmech.2006.01.009
17. Song, W.; Ning, J. & Wang, J. Normal impact of truncated oval-nosed projectiles on stiffened plates. *Int. J. Impact. Eng.*, 2008, **35**(9), 1022-1034. doi:10.1016/j.ijimpeng.2007.05.008
18. Rashid, K.; Abu, A. & Sun, M.K.R. Predicting mesh-independent ballistic limits for heterogeneous targets by a non-local damage computational framework. *Compos. B. Eng*., 2009, **40**(6), 495-510. doi: 10.1016/j.compositesb.2009.03.009
19. Iqbal, M.A.; Gupta, G. & Gupta, N.K. 3D numerical simulations of ductile targets subjected to oblique impact by sharp nosed projectiles. *Int. J Solid. Struct*. 2010, **47**(2), 224-237. doi: 10.1016/j.ijsolstr.2009.09.032
20. Babaei, B.; Shokrieh, M. & Daneshjou, K. The ballistic resistance of multi-layered targets impacted by rigid projectiles. *Mater. Sci. Eng.*, 2011, **530**, 208-217. doi: 10.1016/j.msea.2011.09.076
21. Kidane, B. L. A.; Ravichandran, G. & Ortiz, M. Verification and validation of the optimal transportation mesh free (OTM) simulation of terminal ballistics. *Int. J. Impact. Eng*., 2012, **42**, 25-36. doi: 10.1016/j.ijimpeng.2011.11.003
22. Bonet, J. & Lok, T.S. Variational and momentum preservation aspects of Smooth Particle Hydrodynamic formulations. Comput. *Meth. Appl. Mech. Eng*., 1999, **180** (1-2), 97-115. doi: 10.1016/S0045-7825(99)00051-1
23. Liu, G.R. & Liu, M.B. Smoothed Particle Hydrodynamics a meshfree Particle Method. world scientific Press, 2003. pp. 33-97. doi: 10.1142/9789812564405
24. Liu, M.B.; Liu, G.R. & Lam, K.Y. Constructing Smoothing functions in smoothed particle hydrodynamic with applications. *J. Comput. Appl. Math.*, 2003, **155**(2), 263-284. doi: 10.1016/S0377-0427(02)00869-5
25. Johnson, G. R.; Stryk, R. A.; Holmquist, T. J. & Beissel, S.R. Numerical Algorithms in a Lagrangian Hydrocode Defense Technical Information Center, 1997. pp. 141-155
26. Ulven, C.; Vaidya, U.K. & Hosur, M.V. Effect of projectile shape during ballistic perforation of VARTM carbon/epoxy composite panels. *Compos. Struct.*, 2003, **61**(1-2), 143-150. doi: 10.1016/S0263-8223(03)00037-0
27. Piekutowski, A.J.; Forrestal, M.J.; Poormon, K.L. & Warren, T.L. Perforation of aluminum plates with ogive-nose steel rods at normal and oblique impacts. *Int. J. Impact. Eng*., 1996, **18**(7-8), 877–887. doi: 10.1016/S0734-743X(96)00011-5
28. Steinberg, D.J. Equation of state and strength properties of selected materials, Livermore, California, 1996.
29. Corbett, B.M. Numerical simulations of target hole diameters for hypervelocity impacts into elevated and room temperature bumpers. *Int. J. Impact. Eng.*, 2006, **33**(1-12), 431–440. doi: 10.1016/j.ijimpeng.2006.09.086
30. Johnson, G.R. & Cook.W.H. Fracture characteristics of three metals subjected to various strains, strain rates, temperatures and pressures. *Engng. Fract. Mech.*, 1985, **21**(1), 31-48. doi: 10.1016/0013-7944(85)90052-9
31. Schwer, L.E. Aluminum plate perforation: A comparative case study using Lagrange with erosion, multi-material ALE, and smooth particle hydrodynamics. *In* 7th European LS-DYNA Conference. 2009.
32. Rosenberg, Z.; Kositski, R. & Dekel, E. On the perforation of aluminum plates by 7.62 mm APM2 projectiles. *Int. J. Impact. Eng.*, 2016, **97**, 79–86. doi:10.1016/j.ijimpeng.2016.06.003
33. Abaqus, Abaqus Version 6.14 User's manual, Volume IV: Elements, 2014. pp. 38-82.

CONTRIBUTORS

Mr Ehsan Hedayati received his BSc and MSc in Mechanical Engineering. He holds MS degree in Mechanical Engineering from Islamic Azad University of Saveh, Iran. He has published nearly 10 papers in various journals and conferences. His research interests are : Impact mechanics, composite material, fracture mechanics and finite element method.
In the current study, he is involved in modelling and simulation, literature review, organised reported, organised the study, and drafting of the manuscript.

Dr Mohammad Vahedi received his BS, MS, and PhD in Mechanical Engineering from Amirkabir University of Technology, Shiraz University and Iran University of Science and Technology in Iran, respectively. Currently working as an Assistant Professor and Head of Department of Mechanical Engineering in Faculty of Engineering at Azad University of Saveh, Iran. He has published nearly 20 papers in various journals and conferences. His research interests are vibration and acoustic, impact mechanics, fracture mechanics and finite element method.
In the current study, he is involved in literature review, organised the study and in writing of the manuscript.